



# Limitations in Grain Yield and Carbon Partitioning Differs in Soybean (*Glycine max* (L.) Merr.) Cultivars with Contrasting Photosynthetic Phosphorus-Use Efficiency

Isadora Rodrigues Medina<sup>1,2</sup> · Guilherme Henrique da Rocha<sup>1</sup> · Eduardo Gusmão Pereira<sup>1</sup>

Received: 31 January 2022 / Accepted: 14 July 2022 / Published online: 22 July 2022  
© The Author(s) under exclusive licence to Sociedad Chilena de la Ciencia del Suelo 2022

## Abstract

The aim of the work was to elucidate how different P doses alter photosynthesis and to identify their effects on carbon partitioning and grain production in two soybean cultivars with contrasting photosynthetic phosphorus-use efficiency (PPUE). Two cultivars, UFVS80B10 and TMG7063, were subjected to increasing doses of phosphorus (0.01 mM, 0.1 mM, 0.5 mM, and 1 mM) in Hoagland nutrient solutions. The cultivar with a higher PPUE (TMG7063), presented 24%, 25%, 41%, 46%, and 31% of net photosynthetic rate, stomatal conductance, maximum carboxylation rate of rubisco, electron transport, and triose phosphate use, respectively, than the UFVS80B10 cultivar. However, in both cultivars, there was a reduction in those variables due to the lower P content in the tissues of plants subjected to P deficit. The P deficit caused damage to photosystem II (PSII) only when the plants were close to the R6 stage. The cultivars were efficient in dissipating nonphotochemical energy during P deficit (0.01 mM), but with higher photochemical efficiency in the cultivar TMG7063 at the reproductive stage in higher P doses. The higher absorption of P in the cultivar with low PPUE reflected higher starch and sugar contents in the leaves, stems, and roots, causing a greater biomass gain but with grain yield of 45% lower than the cultivar with the highest PPUE. A higher PPUE in soybean is associated with the maintenance in carbohydrate partitioning under low P, maximizing grain production and presenting photoprotective mechanisms mainly in the grain filling stage.

**Keywords** Triose phosphate use · Carbohydrates · Phosphorus deficit · Chlorophyll *a* fluorescence, Photosynthesis, Rubisco

## 1 Introduction

Phosphorus (P) is an essential nutrient for plant metabolism, and its deficiency is one of the factors that most limit the growth and productivity of soybean crops (He et al. 2017; Zhang et al. 2020). On a global scale, it is estimated that more than half of the agricultural land is deficient in P (Lynch, 2011) and needs fertilizers to ensure crop yield (Macdonald et al. 2011). However, P is obtained almost exclusively from nonrenewable sources, and some optimistic

predictions indicate that P sources could be depleted or extremely reduced in less than 400 years, increasing the costs of obtaining minerals (Veneklaas et al. 2012) also for soybean cultivation.

Soybean occupies approximately 39 million hectares in the Brazilian territory (Embrapa, 2021), with an expected increase of 9.54 million hectares in the next 10 years. Since 1960, P consumption has been increasing in Brazil, and more than 45 million tons have been applied to Brazilian soils. With the expansion of new cultivation areas, P<sub>2</sub>O<sub>5</sub> consumption is estimated to increase in Brazil to 105 million tons by 2050 (Embrapa, 2018). An alternative means of reducing the total amount of phosphate fertilizers applied to crops and contributing to restraining unnecessary agricultural expansion without losing productivity is to develop cultivars with a higher absorption efficiency and internal use of inorganic phosphorus (Pi). There is a significant positive correlation between the efficient use of P and characteristics

✉ Eduardo Gusmão Pereira  
egpereira@ufv.br

<sup>1</sup> Institute of Biological and Health Sciences, Federal University of Viçosa, Highway LMG 818, km 06, s/n, Florestal - MG 35690-000, Brazil

<sup>2</sup> Graduate Program in Plant Physiology, Federal University of Lavras, Lavras, MG, Brazil

related to photosynthesis in soybean, particularly under a P deficit in the soil (Li et al. 2016).

Phosphorus-use efficiency (PUE) can be classified into P absorption efficiency and P internal use efficiency (Iqbal et al. 2019). Absorption efficiency refers to the plant's ability to solubilize P from poorly available sources and/or the absorption of available soluble Pi from the growth medium. The internal efficiency of P use refers to the amount of biomass produced per unit of tissue P, and within it, the photosynthetic P-use efficiency (PPUE) stands out, which refers to the rate of photosynthetic carbon assimilation per unit of P foliar (Hayes et al. 2018).

Increasing photosynthetic efficiency in the use of phosphorus may include remobilization strategies, alteration of organic P fractions, and vacuolar Pi release (Abbas et al. 2018; Ham et al. 2018; Mo et al. 2019). The preferential allocation of P to photosynthetic mesophyll cells is an important feature in species adapted to extremely P-impoorished habitats, contributing to their high PPUE (Hayes et al. 2018). Variation between cultivars for PPUE may be due to differential P uptake characteristics or P distribution patterns within plants (Irf et al. 2020).

The P deficiency reduces photosynthetic capacity by affecting the activities of enzymes involved in the Calvin-Benson cycle and the synthesis of adenosine triphosphate (ATP) and nicotinamide adenine dinucleotide phosphate hydrogen (NADPH) (Lovio-Fragoso et al. 2021). Under conditions of low Pi availability, sucrose synthesis in the cytosol may be restricted, causing decreased triose-P export from the chloroplast, in which more triose-P is retained in the stroma for conversion into starch (Malhotra et al. 2018). The sugars resulting from starch degradation can act as secondary messengers, interacting with phytohormones and regulating the expression of genes that optimize the acquisition of phosphorus in the soil and improve its internal use through morphophysiological changes (Prathap et al. 2022; Zhang et al. 2020), which depend on the photosynthetic capacity of the plant under stress.

Photosynthetic limitations under P deficit are determinants of soybean yield, as observed in the study of Zhang et al. (2014), in which transgenic plants overexpressing acid phosphatase genes increased the PUE without increasing productivity. Therefore, for the selection of soybean cultivars, it is very important to understand how the photosynthetic capacity affects PUE and increases grain production. Although some studies demonstrate how phosphorus deficiency affects soybean growth (Khan et al. 2020; Malhotra et al. 2018; Yan et al. 2015), there is little understanding of the relationship between PUE and photosynthetic characteristics and the consequences in the grain filling stage of soybean. Understanding how photoprotective mechanisms and photosynthetic limitations influence plant tolerance to phosphorus deficiency is the basis for the development

of biotechnological strategies aimed at improving PUE in crops.

It is expected that soybean plants with a higher PUE will have better efficiency in terms of the maximum carboxylation rate of rubisco, triose-P use (TPU), and photoprotective mechanisms and thus be able to maintain carbohydrate accumulation and production under a P deficit. Therefore, the objective of the study was to elucidate how different doses of P limit photosynthesis and to identify their effects on carbon partitioning and biomass on grain production in two soybean cultivars with contrasting photosynthetic phosphorus-use efficiency (PPUE).

## 2 Materials and Methods

### 2.1 Soybean Cultivars and Experimental Conditions

The experiment was conducted from October to January 2018 in a greenhouse at the Universidade Federal de Viçosa (Federal University of Viçosa), Florestal Campus, Brazil (19° 53' 20.23" S e 44° 25' 56.38" W). The mean temperature and relative humidity inside the greenhouse were 26.4 °C and 40.5%, respectively.

Two soybean cultivars were selected for use in this study, UFVS80B10 and TMG7063, optimized for protein and oil production, respectively. Both cultivars have a cycle of approximately 115 days and a high fertility requirement when used in the Cerrado region of Brazil, according to the National Registry of Cultivars (Registro Nacional de Cultivares—RNC).

The seeds were germinated in BOD incubators at a temperature of 25 °C with a photoperiod of 12 h. When the seedlings had developed radicles, but with cotyledons still closed (VE stage; Fig. S1), they were transplanted into 5-L pots without drainage holes, with Hoagland's nutrient solution (Hoagland and Arnon, 1950) with four P concentrations (0.01 mM, 0.1 mM, 0.5 mM, and 1 mM), according to Table S1. The P doses were selected based on the literature (Win et al. 2010). The control treatment corresponded to the recommended dose of 1 mM. The pots were filled daily with deionized water, and the pH was measured every 2 days and adjusted to 5.5. The nutrient solution was changed weekly. Oxygenation of the roots was performed with air at a flow rate of 80 L/h for 10 min 12 times a day.

### 2.2 Evaluation of the Photosynthetic Metabolism

Periodic measurements of chlorophyll *a* fluorescence were carried out between the V2 and R7 stages with a pulse-modulated fluorometer Mini-PAM (Heinz Walz, Effeltrich, Germany). The measurements were performed on the central leaflet of the third fully expanded leaf from

the apex. In the pre-dawn, the minimum fluorescence ( $F_0$ ) and maximum fluorescence ( $F_m$ ) were measured in dark-acclimated leaves. The values obtained were used to determine the maximum quantum efficiency of photosystem II (PSII) ( $F_v/F_m = (F_m - F_0)/F_m$ ) (Genty et al., 1989). After determining  $F_v/F_m$ , the plant tissue was exposed for 30 s to a photosynthetic photon flux density (PPFD) of  $1000 \mu\text{mol m}^{-2} \text{s}^{-1}$ , and then a saturating light pulse was applied. From this process, the following variables were determined:  $F$ , the fluorescence in a *steady state* before the saturating light pulse; and  $F_m'$ , the maximum fluorescence of the illuminated plant tissue. The following variables were calculated:  $\phi_{\text{PSII}} = (F_m' - F)/F_m'$ , the effective quantum yield of PSII in the illuminated plant tissue;  $\phi_{\text{NPQ}} = F/F_m' - F/F_m$ , the quantum yield of regulated nonphotochemical energy loss in PSII (Genty and Harbinson, 1996);  $\phi_{\text{NO}} = F/F_m$ , the quantum yield of nonregulated nonphotochemical energy loss in PSII (Genty and Harbinson, 1996);  $\text{NPQ} = F_m - F_m'/F_m'$ , the nonphotochemical fluorescence quenching (Bilger and Björkman 1990); and  $\text{ETR} = \phi_{\text{PSII}} \times \text{PPFD} \times \alpha$ , the electron transport rate, where  $\alpha$ , defined as 0.47 for soybean (Gallé et al. 2013), is the product of leaf absorptance and the proportions of photons destined for the two photosystems (Melis et al. 1987).

The chlorophyll *a*, chlorophyll *b*, chlorophyll *a/b* ratio, and total chlorophyll indices were evaluated simultaneously with the fluorescence measurements using a ClorofiLOG portable chlorophyll meter (Falker, Brazil). Three measurements were made at each central leaflet from among the same leaves used for fluorescence measurements of chlorophyll *a*.

At the grain filling stage (R5), gas exchange measurements were performed on the third fully expanded leaf using an infrared gas analyzer (IRGA; LI-6400XT, Li-Cor Inc., Lincoln, NE, USA). The following variables were obtained: net photosynthetic rate ( $A$ ), stomatal conductance ( $g_s$ ), transpiration ( $E$ ), and the ratio between internal and external  $\text{CO}_2$  concentrations ( $C_i/C_a$ ). The controlled conditions in the cuvette included a  $\text{CO}_2$  concentration of  $400 \mu\text{mol CO}_2 \text{mol}^{-1}$ , an irradiance of  $1200 \mu\text{mol m}^{-2} \text{s}^{-1}$ , a temperature of  $28^\circ\text{C}$ , and a humidity of 60%.

Additionally, in R5,  $\text{CO}_2$  response curves ( $A/C_i$ ) were performed in the central leaflets of the third fully expanded leaf. The measurements were made at different levels of  $\text{CO}_2$  (400, 300, 200, 100, 50, 400, 500, 600, 700, 800, 1000, 1200, and  $1300 \mu\text{mol CO}_2 \text{mol}^{-1}$ ). The minimum time required to stabilize the reading at each concentration was 60 s, and the maximum time was 120 s. The data obtained in the curves were used to calculate the maximum carboxylation rate of rubisco ( $V_{\text{cmax}}$ ), electron transport ( $J$ ), and triose phosphate use ( $TPU$ ) (Sharkey et al. 2007).

## 2.3 Quantification of Phosphorus in Tissues

The quantification of P was performed in dry samples (0.15 g) from each organ. One leaf from each replicate was collected at stage R5, and stems and roots were collected at stage R8. The methodology of Embrapa (1997) was used with some modifications; the digestion mixture was composed of copper sulfate and sodium sulfate at a ratio of 1:10 and 3 mL of concentrated sulfuric acid. The cocktail solution contained ammonium molybdate and ascorbic acid.

PPUE was calculated from the net photosynthetic rate per unit of leaf mass ( $A$  mass) and its phosphorus content.

## 2.4 Analysis of Carbohydrates

Carbohydrates were determined in leaves collected at stage R7 and roots and stems collected at stage R8. Samples (0.5 g) of dried and ground plant materials were homogenized in a mortar with 5 ml of boiling 80% ethyl alcohol for extraction. This process was performed twice.

The pellet was used for the determination of starch (AS) according to Hodge (1962), and the supernatant from the extraction was used for the quantification of reducing sugars (RS) according to (Miller 1959) and for the quantification of total soluble sugars (TSS) according to Dubois et al. (1956). The nonreducing sugars (NRS) were determined by the difference in TSS-RS.

## 2.5 Morphological Evaluations

At stage R5, two trifoliate leaves were removed from each plant and scanned, and the leaf area was determined using ImageJ software. The same trifoliate leaves were dried in a forced-air oven for 72 h at  $65^\circ\text{C}$  and then weighed to calculate the dry biomass. From these data, the leaf dry mass per unit leaf area (LMA,  $\text{g cm}^{-2}$ ) was calculated.

At the R8 stage, the plants were sectioned into roots, grains, pods, leaves, and stems, which were separately placed in paper bags, placed in a forced-air oven for 72 h at  $65^\circ\text{C}$ , and subsequently used to obtain the dry mass (g).

## 2.6 Experimental Design and Statistical Analysis

The experiment was conducted in randomized blocks with five replicates in a  $4 \times 2$  factorial scheme, with four doses of P supplied in the nutrient solution (0.01 mM, 0.1 mM, 0.5 mM, and 1 mM) for two cultivars (UFVS80B10 and TMG7063).

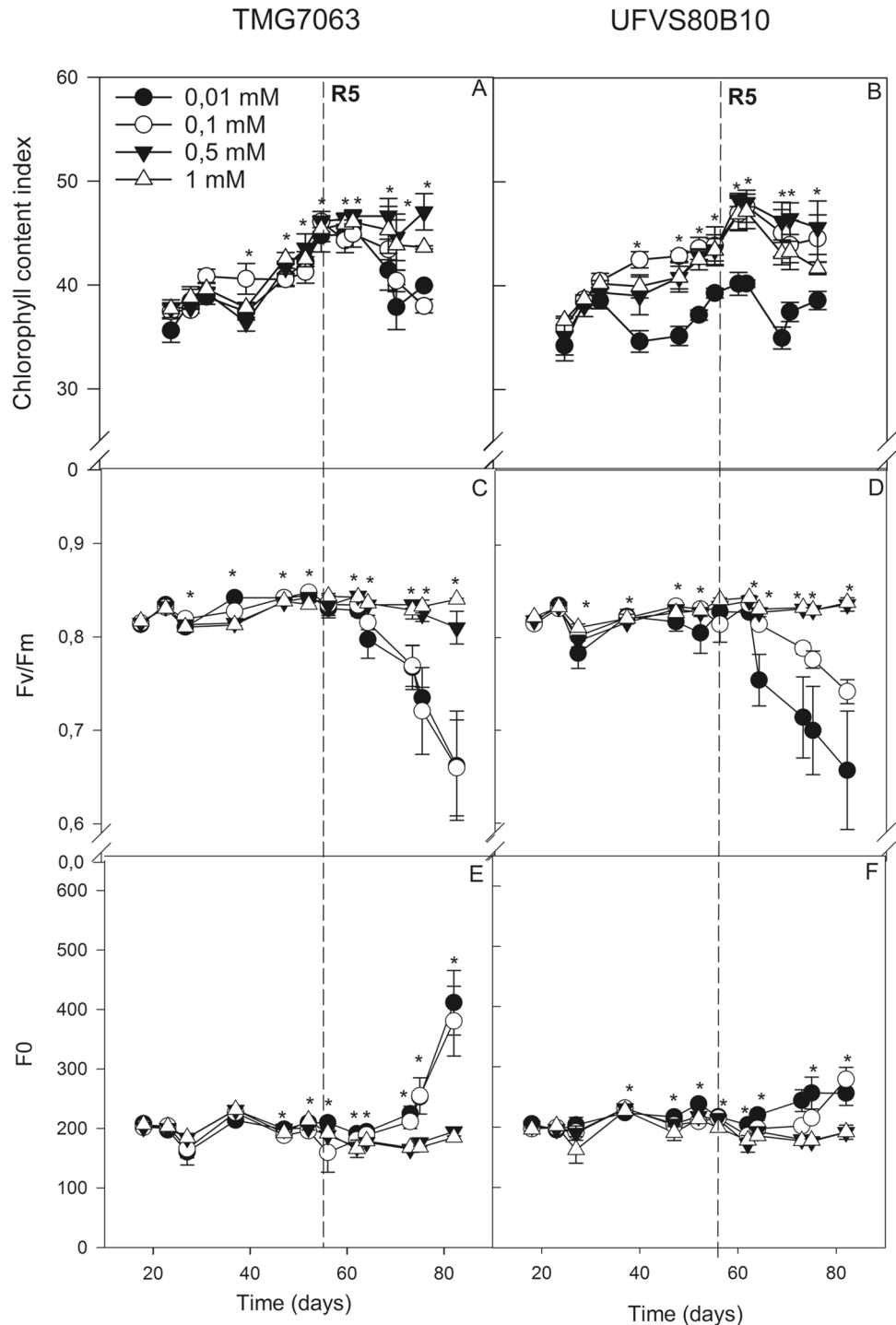
To meet the assumptions of two-way ANOVA, the  $C_i/C_a$  data were transformed to  $\sqrt{X}$ , and the available starch (AS) and sugars (RS, TSS, and NRS) data were transformed to  $\log X$ . The data were subjected to regression analysis using SigmaPlot 14.0 software. The Equations and coefficient of

determination of the regressions of cultivars are presented in chart S1. The correlation analysis was performed using the statistical software R (version 3.5.1). The correlation and significance between variables are in Fig. S9. The chlorophyll data and chlorophyll *a* fluorescence over time were subjected to a repeated-measures ANOVA followed by the Tukey test ( $p < 0.05$ ) using the statistical program R (version 3.5.1).

### 3 Results

The P deficit resulted in lower total chlorophyll (Fig. 1a), chlorophyll *a*, and chlorophyll *b* (Fig. S2) values only at the grain filling stage in the TMG7063 cultivar subjected to doses of 0.01 mM and 0.1 mM. However, the plants of the cultivar UFVS80B10 subjected to a dose of 0.01 mM

**Fig. 1** Chlorophyll content index (A and B), maximum quantum yield of PSII (Fv/Fm; C and D), and initial fluorescence (F0; E and F) of cultivars TMG7063 (A, C, E) and UFVS80B10 (B, D, F), over time of exposure to doses of 0.01 mM, 0.1 mM, 0.5 mM, and 1 mM of P in nutrient solution. Asterisks represent a statistical difference between treatments ( $p < 0.05$ ) by the Tukey test. Values are the means  $\pm$  standard error ( $n = 5$ )



showed earlier reductions in total chlorophyll (Fig. 1B), chlorophyll *a*, and chlorophyll *b* (Fig. S2), in vegetative stage V6.

The P deficit (at doses of 0.01 mM and 0.1 mM) reduced the Fv/Fm values in both cultivars from grain filling and maturation stages, respectively (Fig. 1C and D). When subjected to the highest doses of phosphorus (0.5 mM and 1 mM), both cultivars showed no significant differences in Fv/Fm (Fig. 1C and D) and F0 (Fig. 1E and F) over time. No differences ( $p < 0.05$ ) were observed in the F0 up to the V6 stage in plants of both cultivars exposed to different doses of phosphorus (Fig. 1E and F). During the pod expansion stages, the UFVS80B10 cultivar had a higher F0 than the TMG7063 cultivar at a dose of 0.01 mM. At the beginning of grain filling, the plants of both cultivars subjected to the lowest doses of P showed an increase in F0, with greater values in cultivar TMG7063 than the cultivar UFVS80B10 at the end of the cycle.

In both cultivars, the plants exposed to 0.01 mM P showed the lowest *A* values in stage R5, followed by the plants exposed to 0.1 mM P. The cultivation of plants at doses of 0.5 mM and 1 mM showed no significant difference in *A* (Fig. 2A). The TMG7063 cultivar showed higher *A* values than the UFVS80B10 cultivar at all P levels (Fig. 2A). Photosynthesis showed a negative correlation with  $\phi_{\text{NPQ}}$  ( $r = -0.5429$ ) but a positive correlation with the grain dry matter (GDM) ( $r = 0.5661$ ) (Fig. S9).

Cultivar TMG7063 had a higher PPUE than cultivar UFVS80B10 (Fig. 2B). The highest P dose (1 mM) resulted in the lowest PPUE in both cultivars, with no difference between them.

The cultivar UFVS80B10 showed no differences in *E* values between plants with different doses of P. However, the lowest dose of P reduced the *E* in the cultivar TMG7063 (Fig. 2C). The P deficits did not result in a significant decrease in  $g_s$ , with the highest values observed for cultivar TMG7063 (Fig. 2D).

There was a decrease in Ci/Ca in cultivar UFVS80B10 when cultivated with the highest doses of P. The TMG7063 cultivar did not change the Ci/Ca values in response to different P doses (Fig. 2E).

Both cultivars presented an increase in the values of  $V_{\text{cmax}}$ , *J*, and *TPU* with increases in the phosphorus dose up to 0.5 mM (Fig. 2F, G, H). Cultivar TMG7063 showed  $V_{\text{cmax}}$ , *J*, and *TPU* values higher than those of the UFVS80B10 cultivar to all phosphorus doses (Fig. 2F, G, H). The *TPU* values had a significant positive correlation with photosynthesis ( $r = 0.4730$ ) (Fig. S9).

The TMG7063 cultivar showed higher  $\phi_{\text{PSII}}$  than UFVS80B10 at P doses of 1 mM, 0.5 mM, and 0.1 mM, with lower values in plants subjected to a dose of 0.01 mM in R5 (Fig. S3). The values of  $\phi_{\text{NPQ}}$  and  $\phi_{\text{NO}}$  (Fig. S3) did not differ as a function of the cultivar. Plants grown at a P

dose of 0.01 mM had the highest  $\phi_{\text{NPQ}}$  and NPQ, followed by those grown with 0.1 mM dose. The UFVS80B10 cultivar showed the highest  $\phi_{\text{NO}}$  at a dose of 0.5 mM, differing from plants at the lowest P dose. The  $\phi_{\text{NO}}$  of cultivar TMG7063 did not change with the different P doses (Fig. S3). Both cultivars subjected to the lower P dose had reduced ETR, not only at the R5 stage (Fig. S5) but throughout the entire cycle (Fig. S6). Only at the beginning of grain maturation did the plants grown with 0.1 mM P also showed a decrease in  $\phi_{\text{PSII}}$  and ETR values (Figs. S4 and S6).

The cultivars exhibited increased accumulation of starch and TSS in the leaves and roots up to a dose of 0.5 mM (Fig. 3A, B). Except for the roots (Fig. 3C, D), the cultivar UFVS80B10 showed higher AS and TSS contents (Fig. 3A, B) and NRS and RS contents (Fig. S7) than the TMG7063 cultivar at all P doses.

The increase in P in the nutrient solution resulted in its linear uptake in the leaves of both cultivars (Fig. 4A), with higher values in the UFVS80B10 cultivar than in TMG7063. In the roots, there was a significant increase in P content up to a dose of 0.5 mM for both cultivars (Fig. 4B).

The leaf dry matter (LDM) and root dry matter (RDM) (Fig. 4C, D) were lower in plants exposed to 0.01 mM and higher in those exposed to 0.1, 0.5, and 1 mM regardless of cultivar. In both cultivars, the plants subjected to the lowest doses of P (0.01 mM and 0.1 mM) showed the lowest gains in GDM and total dry matter (TDM) (Fig. 4E, F). The UFVS80B10 cultivar showed greater gains in TDM, LDM, and RDM than did the TMG7063 cultivar; however, the greatest gain in GDM (Fig. 4E) was observed for the TMG7063 cultivar.

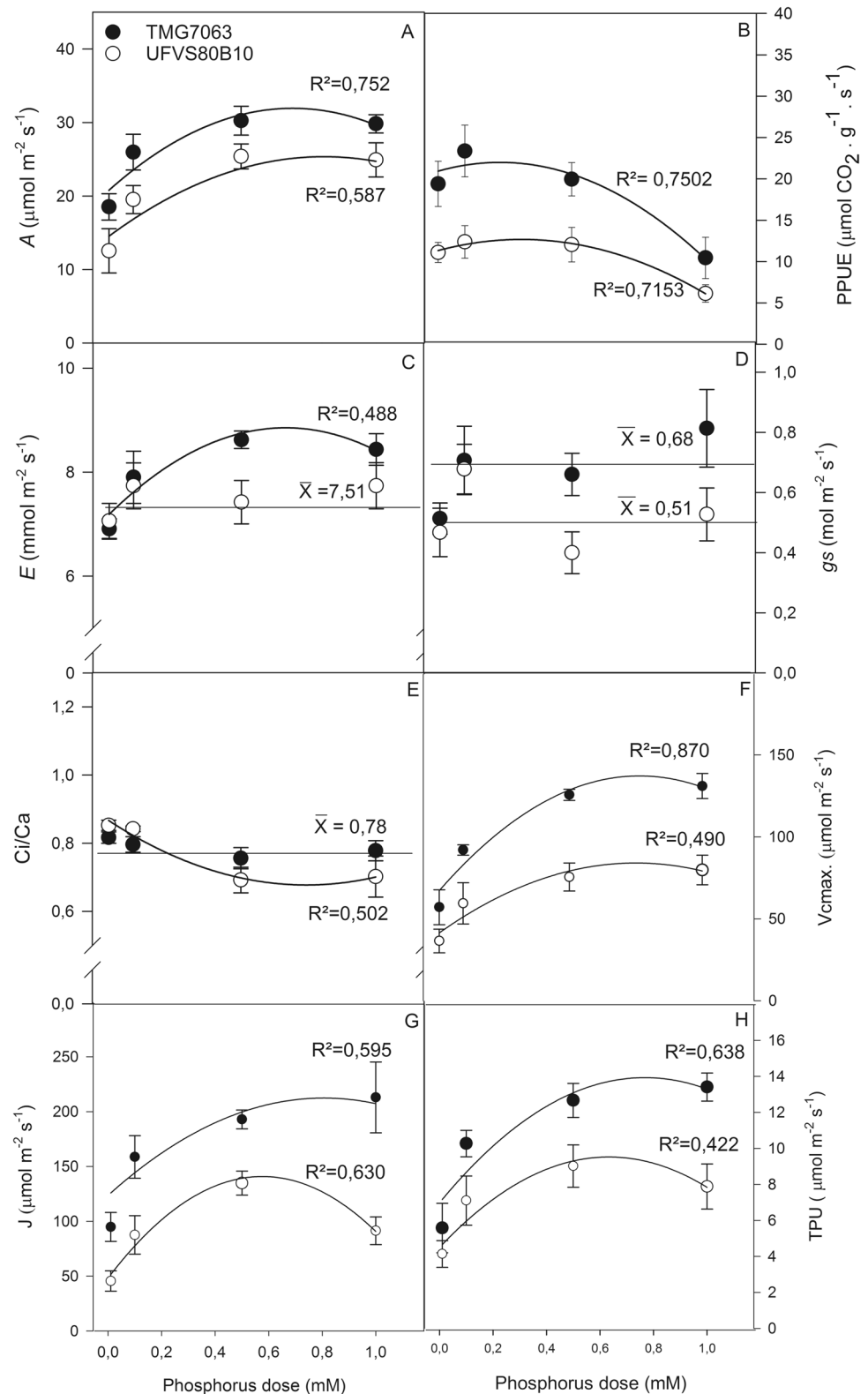
The plants of both cultivars exhibited decreased root/shoot ratios as the phosphorus dose increased (Fig. S8).

## 4 Discussion

The soybean crop is sensitive to P deficiency. The main causes of the differences in PPUEs between the cultivars were due to the efficiency in carboxylation and light-use mechanisms coupled with low P requirement. The greater carboxylation capacity, RuBP regeneration, and export of triose-P in the cultivar TMG7063 contributed to its higher PPUE. As a consequence, in the grain filling stage, P deficiency caused severe damage to the photosynthetic apparatus of the cultivar UFVS80B10, as evidenced by the permanent decrease in Fv/Fm.

The carbon partitioning in favor of starch observed in the TMG7063 cultivar may have contributed to the reduction in photosynthesis by inhibition by the final product (Malhotra et al. 2018). However, starch accumulation served as a source of sugars in the grain filling stage, contributing to the grain production and quality in the cultivar

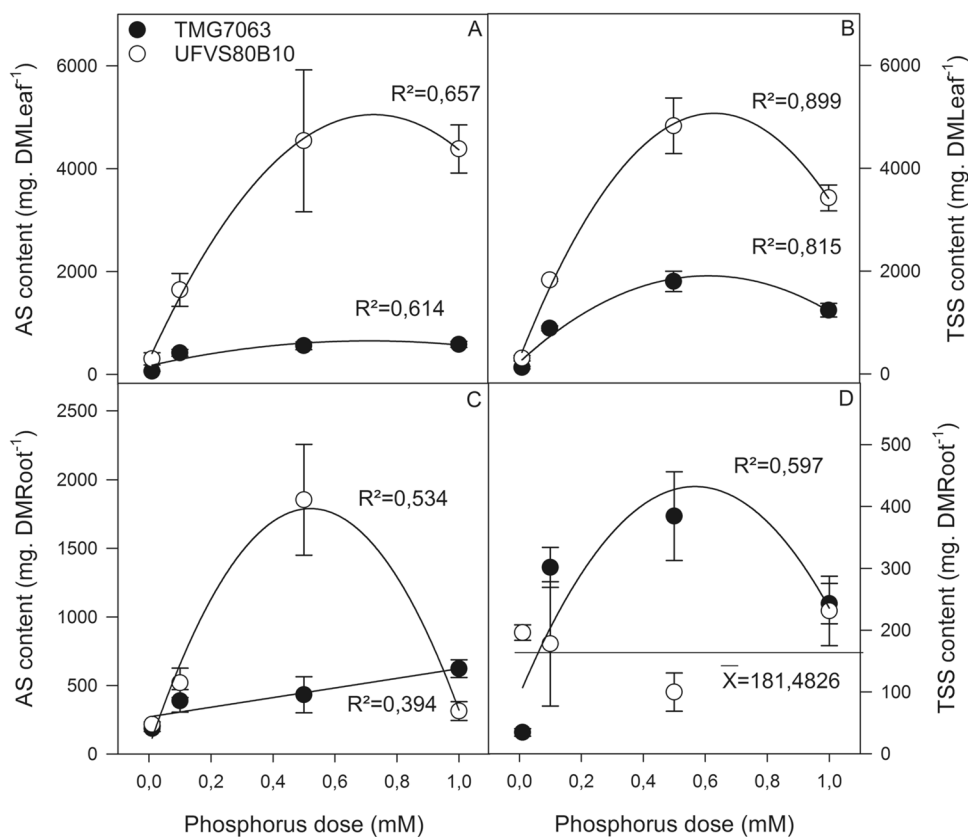
**Fig. 2** Net photosynthesis (**A**), photosynthetic phosphorus-use efficiency (PPUE; **B**), transpiration ( $E$ ; **C**), stomatal conductance ( $g_s$ ; **D**), ratio of intercellular to ambient  $\text{CO}_2$  concentrations ( $C_i/C_a$ ; **E**), maximum rate of rubisco carboxylation ( $V_{cmax}$ ; **F**), maximum rate of electron transport ( $J$ ; **G**), triose phosphate utilization (TPU; **H**) of cultivars TMG7063 and UFVS80B10, at the grain filling stage (R5) after exposure to doses of 0.01 mM, 0.1 mM, 0.5 mM, and 1 mM of P in nutrient solution. Values are the means  $\pm$  standard error ( $n=5$ ). The regression equations are found in the supplementary chart S1



with higher PPUE. Limitations in the metabolism of triose-P for sucrose synthesis may delay Pi recycling and RuBP regeneration (Yang et al. 2016). The reduction in RuBP regeneration in the photosynthetic process of plants

exposed to low P may be the result of the greater use of sugar phosphates from chloroplasts in starch biosynthesis (MacNeill et al. 2017). A reduction in the amount of rubisco has been reported to balance the regeneration

**Fig. 3** Starch content in leaf and root (AS; **A** and **C**), total soluble sugars content in leaf and root (TSS; **B** and **D**) of cultivars TMG7063 and UFVS80B10, after exposure to doses of 0.01 mM, 0.1 mM, 0.5 mM, and 1 mM of P in nutrient solution. Values are the means  $\pm$  standard error ( $n = 5$ ). The regression equations are found in the supplementary chart S1



capacity of RuBP when plants are under P deficit (Poudyal et al. 2021).

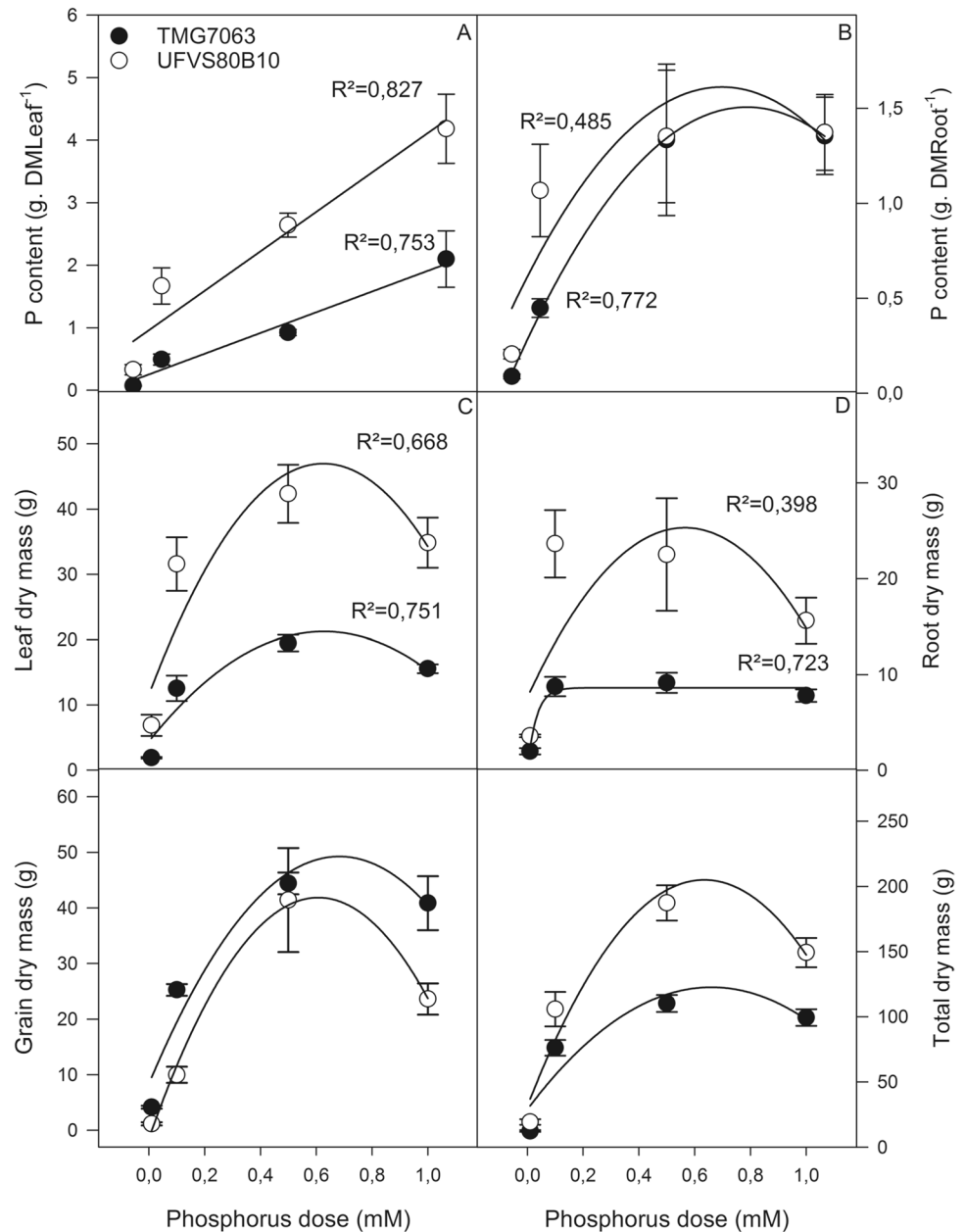
Despite the effects of low P on the amount of rubisco, the reductions in  $V_{\text{cmax}}$  and  $J$  values at the lowest P doses might have occurred as a consequence of decreases in its activation state and the amount of rubisco (Singh et al. 2019), as a function of  $TPU$  limitation over time (Yang et al., 2016). The activation of rubisco by the enzyme rubisco activase (RCA) requires the hydrolysis of ATP (Waheeda et al. 2022); therefore, with lower energy production under P deficit, rubisco activation may be lower. In addition, P deficiency reduces the expression of RCA genes (such as *GmRCA $\beta$* ) that are associated with P efficiency in soybean (Chu et al. 2018). Another potential limitation of RuBP regeneration is the lower activity of enzymes in the Calvin-Benson cycle that also depend on ATP, such as 3-phosphoglycerate kinase, NADP-glyceraldehyde-3-phosphate dehydrogenase, sedoheptulose-1,7-bisphosphate phosphatase, and ribulose-5-phosphate kinase (Tantray et al. 2020).

An increased NPQ value is important for the performance of soybean cultivars under phosphorus deficit. The reduction in ATP synthase activity in low P stress limits the export of protons to the chloroplast stroma, acidifying the lumen. With this process occurs a reduction in ETR under P deficiency (Carstensen et al. 2018), as also observed in this study and the reduction in lumen pH activates the NPQ

components. The dissipation of excess energy may be related to the xanthophyll cycle, in which the zeaxanthin, converted from violaxanthin, can dissipate excess energy and protects the photosystems from overexcitation and possible damage (Li et al. 2018). The cultivars were efficient in dissipating nonphotochemical energy to avoid damaging PSII until the beginning of stage R5, as observed by the values of  $\phi_{\text{NO}}$  and  $F_v/F_m$ . As the processes of  $\phi_{\text{NPQ}}$ ,  $\phi_{\text{NO}}$ , and  $\phi_{\text{PSII}}$  are competitive with each other, the increases in the values of  $\phi_{\text{NPQ}}$  over time resulted in a reduction in the values of  $\phi_{\text{NO}}$  and  $\phi_{\text{PSII}}$  in plants under P deficit. This result means that most of the absorbed energy was dissipated rather than used in the photosynthetic process.

In both cultivars studied, the P deficits under doses of 0.01 mM and 0.1 mM began to cause severe effects in the plants near the R6 stage, according to the  $F_v/F_m$ , chlorophyll index, and  $F_0$  data. Photoinhibition at the end of the cycle was confirmed by the reduction in  $F_v/F_m$  and the increases in  $F_0$  and  $\phi_{\text{NO}}$  in plants exposed to the lowest doses of P, indicating a reduction in the capacity of energy transfer from the antenna complex to the reaction centers (El-Mejjaouy et al. 2022). The higher  $F_0$  values and lower  $\phi_{\text{NPQ}}$  values of cultivar TMG7063 than UFVS80B10 highlighted the different strategies between the cultivars; UFVS80B10 showed a reduction in the chlorophyll index from the V6 stage, when  $F_v/F_m$  had not yet

**Fig. 4** P content in the leaf (A) and root (B), dry mass of leaf (C) and root (D), grain dry mass (E), total dry mass (F) of cultivars TMG7063 and UFVS80B10, after exposure to doses of 0.01 mM, 0.1 mM, 0.5 mM, and 1 mM of P in nutrient solution. Values are the means  $\pm$  standard error ( $n=5$ ). The regression equations are found in the supplementary chart S1



been affected, which resulted in a reduction of the amount of light collected by the antenna complex. The increase in F0 is related to the photodamage caused by the inability to transfer excitation energy to the PSII reaction center during grain filling.

With the increase in the demand for phosphorus at the end of the cycle, the TMG7063 cultivar began to degrade stored starch, which avoids compromising seed formation. Therefore, from the R7 stage, an increase in TSS/AS ratio was observed in plants subjected to doses of 0.1 mM, 0.5 mM, and 1 mM P. Sugars can also act as secondary messengers, aiding in the expression of genes in response to phosphorus deficit (Prathap et al. 2022).

The detrimental effects of the lower P dose (0.01 mM) on the photosynthesis of both cultivars were highlighted by the insufficient carbohydrates produced for storage and use in the stages of higher demand for photoassimilates. Activation of starch degradation under abiotic stress seems to be a common response among plants (Thalmann and Santelia 2017). Plants under stress during grain filling can degrade more starch sources in their vegetative tissues to complete seed development (MacNeill et al. 2017). The higher NRS than RS values indicate high sucrose levels, also suggesting starch degradation. Once generated, leaf sucrose can be translocated to sink tissues. High sucrose content in the phloem acts as a signal for induction of gene



expression, which results in better P absorption by increasing inorganic phosphate transporters and the secretion of acid phosphatases and organic acids that release more P from the soil (Zogli et al. 2017). Therefore, the increase in NRS in the stem and the increase in starch in the roots may be a consequence of the translocation of sucrose via the phloem to the roots, where it was stored as starch. Although the mechanism is different between species, it is believed that translocation occurs through the mass flow model (Pang et al. 2018). This idea can apply in our study because the lower dose of P resulted in lower transpiration, which may have led to a lower accumulation of P in the shoots of plants and consequently caused lower production of carbohydrates.

The reduction in transpiration was not related to significant changes in *g<sub>s</sub>* but may be linked to increased mesophilic resistance under severe phosphorus restriction. According to Singh et al. (2019), a reduction in mesophilic conductance may restrict the diffusion of CO<sub>2</sub> to carboxylation sites, which is directly related to the decrease in *V<sub>max</sub>* values at the lowest dose of P. Therefore, the increase in the *C<sub>i</sub>/C<sub>a</sub>* ratio was not due to increased CO<sub>2</sub> diffusion but most likely due to the reduced carboxylation capacity of rubisco. The LMA results corroborate the hypothesis of mesophilic limitation and are similar to the findings of Chu et al. (2018). Soybean leaves grown under P deficit are generally smaller and thicker, with fewer chloroplasts and thinner thylakoid stacks than leaves of plants with adequate P supply (Chu et al. 2018). Jacob and Lawlor (1991) also found that mesophilic factors were more limiting than stomatal factors to the photosynthesis of soybean plants subjected to a P deficit.

P deficiency leads to an increase in the allocation of carbohydrates to the roots (Prathap et al. 2022), which may explain the increase in root/shoot ratio with increased AS accumulation. This shift in carbohydrate allocation is a strategy of many plants under P limitation, such as common bean (García-Caparrós et al. 2021), cotton (Singh et al. 2013), and other soybean cultivars (Chu et al. 2018). Plants acclimate to nutritional deficiency by allocating more resources to the organs involved in acquiring these nutrients, which directly influences their biomass (Yang et al. 2020).

The higher carbohydrate content in the UFVS80B10 cultivar than the TMG7063 cultivar is directly related to its higher P content in all tissues, evidencing its efficient phosphorus absorption, but with lower PPUE. The efficiency in the use of internal P is generally lower in plants with a high P acquisition efficiency as a result of higher concentrations of P in the tissue (Rose et al. 2016). The UFVS80B10 cultivar invested the P absorbed in carbohydrates for vegetative growth and therefore showed greater stem lengths and diameters and TDM, LDM, stem dry matter (SDM), and RDM values. The higher PPUE in cultivar TMG7063 allowed more investment in grain production.

## 5 Conclusions

The cultivar with higher photosynthetic efficiency in the use of phosphorus (P) showed higher values of maximum carboxylation rate of rubisco, electron transport, and triose phosphate use with lower amounts of P in the tissues. The reductions in maximum carboxylation rate of rubisco and electron transport at lower P doses may be a consequence of triose phosphate use limitation over time, resulting in decreased regeneration of ribulose-1,5-bisphosphate (RuBP) and lower rubisco carboxylase activity.

The P deficit favored starch synthesis in the cultivar with lower photosynthetic phosphorus-use efficiency (PPUE), causing inhibition of photosynthesis by the final product. The photosynthesis of the cultivar with lower PPUE was reduced by energy metabolism resulting from lower adenosine triphosphate production under P deficit.

Under P deficit, the nonphotochemical dissipation mechanisms were important to avoid photoinhibition until the grain filling stage. However, for both cultivars studied, the P deficit started to damage photosystem II when the plants were between the grain filling and maturation stages, as observed by the reduction in maximum quantum efficiency of photosystem II values and chlorophyll indices.

This information about photosynthetic responses of soybean plants to low P could be useful in breeding strategies, mainly by using maximum quantum efficiency of photosystem II, maximum carboxylation rate of rubisco, electron transport, and triose phosphate use as selection tools.

**Supplementary Information** The online version contains supplementary material available at <https://doi.org/10.1007/s42729-022-00940-7>.

**Funding** IRM received a scholarship from the Coordenação de Aperfeiçoamento de Pessoal de Nível Superior – Brasil (CAPES) – Finance Code 001. EG Pereira is a recipient of a research productivity grant from the National Council for Scientific and Technological Development (CNPq).

**Data Availability** The datasets generated during the current study are available from the corresponding author on reasonable request.

## Declarations

**Conflict of Interest** The authors declare no competing interest.

## References

- Abbas M, Shah JA, Irfan M, Memon MY (2018) Remobilization and utilization of phosphorus in wheat cultivars under induced phosphorus deficiency. *J Plant Nutr* 41:1522–1533. <https://doi.org/10.1080/01904167.2018.1458871>

- An-cheng LUO, Assan MJH, Xing-hua WEI (2006) Effect of phosphorus deficiency on leaf photosynthesis and carbohydrates partitioning in two rice genotypes with contrasting low phosphorus susceptibility. *Rice Sci* 13:283–290
- Bilger W, Björkman O (1990) Role of the xanthophyll cycle in photo-protection elucidated by measurements of light-induced absorbance changes, fluorescence and photosynthesis in leaves of *Hedera canariensis*. *Photosynth Res* 25:173–185. <https://doi.org/10.1007/bf00033159>
- Carstensen A, Herdean A, Schmidt SB, Sharma A, Spetea C, Pribil M, Husted S (2018) The impacts of phosphorus deficiency on the photosynthetic electron transport chain. *Plant Physiol* 177:271–284. <https://doi.org/10.1104/pp.17.01624>
- Dubois M, Gilles KA, Hamilton JK, Rebers PA, t, Smith F. (1956) Colorimetric method for determination of sugars and related substances. *Anal Chem* 28:350–356
- Gallé A, Lautner S, Flexas J, Ribas-Carbo M, Hanson D, Roesgen J, Fromm J (2013) Photosynthetic responses of soybean (*Glycine max* L.) to heat-induced electrical signalling are predominantly governed by modifications of mesophyll conductance for CO<sub>2</sub>. *Plant, Cell Environ* 36:542–552. <https://doi.org/10.1111/j.1365-3040.2012.02594.x>
- García-Caparrós P, Lao MT, Preciado-Rangel P, Sanchez E (2021) Phosphorus and carbohydrate metabolism in green bean plants subjected to increasing phosphorus concentration in the nutrient solution. *Agronomy* 11(2):245. <https://doi.org/10.3390/agronomy11020245>
- Genty B, Briantais J-MM, Baker NR (1989) The relationship between the quantum yield of photosynthetic electron transport and quenching of chlorophyll fluorescence. *Biochim Biophys Acta*. 990(1):87–92. [https://doi.org/10.1016/S0304-4165\(89\)80016-9](https://doi.org/10.1016/S0304-4165(89)80016-9)
- Ham BK, Chen J, Yan Y, Lucas WJ (2018) Insights into plant phosphate sensing and signaling. *Curr Opin Biotechnol* 49:1–9. <https://doi.org/10.1016/j.copbio.2017.07.005>
- Hayes PE, Clode PL, Oliveira RS, Lambers H (2018) Proteaceae from phosphorus-impooverished habitats preferentially allocate phosphorus to photosynthetic cells: an adaptation improving phosphorus-use efficiency. *Plant Cell Environ* 41:605–619. <https://doi.org/10.1111/pce.13124>
- He J, Jin Y, Du Y-L, Wang T, Turner NC, Yang R-P, Siddique KHM, Li F-M (2017) Genotypic variation in yield, yield components, root morphology and architecture, in soybean in relation to water and phosphorus supply. *Front Plant Sci* 8:1–11. <https://doi.org/10.3389/fpls.2017.01499>
- Iqbal A, Gui H, Zhang H, Wang X, Pang N, Dong Q, Song M (2019) Genotypic variation in cotton genotypes for phosphorus-use efficiency. *Agronomy* 9(11):689. <https://doi.org/10.3390/agronomy9110689>
- Jacob J, Lawlor DW (1991) Stomatal and mesophyll limitations of photosynthesis in phosphate deficient sunflower, maize and wheat plants. *J Exp Bot* 42:1003–1011
- Khan BA, Hussain A, Elahi A, Adnan M, Amin MM, Toor MD, Aziz A, Sohail MK, Wahab A, Ahmad R (2020) Effect of phosphorus on growth, yield and quality of soybean (*Glycine max* L.); A review. *Int J Appl Res* 6:540–545
- Li H, Yang Y, Zhang H, Chu S, Zhang X (2016) A Genetic Relationship between Phosphorus Efficiency and Photosynthetic Traits in Soybean as Revealed by QTL Analysis Using a High-Density Genetic Map 7:1–16. <https://doi.org/10.3389/fpls.2016.00924>
- Li P, Weng J, Zhang Q, Yu L, Yao Q, Chang L, Niu Q (2018) Physiological and biochemical responses of *Cucumis melo* L. chloroplasts to low-phosphate stress. *Front Plant Sci* 871:1–13. <https://doi.org/10.3389/fpls.2018.01525>
- Lovio-Fragoso JP, de Jesús-Campos D, López-Elías JA, Medina-Juárez LÁ, Fimbres-Olivarría D, Hayano-Kanashiro C (2021) Biochemical and molecular aspects of phosphorus limitation in diatoms and their relationship with biomolecule accumulation. *Biology (basel)* 10:1–21. <https://doi.org/10.3390/biology10070565>
- Lynch JP (2011) Root Phenotypes for Enhanced Soil Exploration and Phosphorus Acquisition: Tools for Future Crops 156:1041–1049. <https://doi.org/10.1104/pp.111.175414>
- Macdonald GK, Bennett EM, Potter PA, Ramankutty N (2011) Agronomic phosphorus imbalances across the world's croplands. *108(7):3086–3091*. <https://doi.org/10.1073/pnas.1010808108>
- MacNeill GJ, Mehrpouyan S, Minow MAA, Patterson JA, Tetlow IJ, Emes MJ (2017) Starch as a source, starch as a sink: the bifunctional role of starch in carbon allocation. *J Exp Bot* 68:4433–4453. <https://doi.org/10.1093/jxb/erx291>
- Melis A, Spangfort M, Andersson B (1987) Light-absorption and electron-transport balance between photosystem II and photosystem I in spinach chloroplasts. *Photochem Photobiol* 45:129–136. <https://doi.org/10.1111/j.1751-1097.1987.tb08413.x>
- Miller GL (1959) Use of dinitrosalicylic acid reagent for determination of reducing sugar. *Anal Chem* 31:426–428. <https://doi.org/10.1021/ac60147a030>
- Mo Q, Li Z, Sayer EJ, Lambers H, Li Y, Zou B, Tang J, Heskell M, Ding Y, Wang F (2019) Foliar phosphorus fractions reveal how tropical plants maintain photosynthetic rates despite low soil phosphorus availability. *Funct Ecol* 33:503–513. <https://doi.org/10.1111/1365-2435.13252>
- Pang J, Zhao H, Bansal R, Bohuon E, Lambers H, Ryan MH, Siddique KHM (2018) Leaf transpiration plays a role in phosphorus acquisition among a large set of chickpea genotypes. *Plant Cell Environ* 41:2069–2079. <https://doi.org/10.1111/pce.13139>
- Parry MAJ, Keys AJ, Madgwick PJ, Carmo-Silva AE, Andralojc PJ (2008) Rubisco regulation: a role for inhibitors. *J Exp Bot* 59:1569–1580. <https://doi.org/10.1093/jxb/ern084>
- Prathap V, Kumar A, Maheshwari C, Tyagi A (2022) Phosphorus homeostasis: acquisition, sensing, and long-distance signaling in plants. *Mol Biol Rep*. <https://doi.org/10.1007/s11033-022-07354-9>
- Rose TJ, Mori A, Julia CC, Wissuwa M (2016) Screening for internal phosphorus utilisation efficiency: comparison of genotypes at equal shoot P content is critical. *Plant Soil* 401:79–91. <https://doi.org/10.1007/s11104-015-2565-7>
- Sharkey TD, Bernacchi CJ, Farquhar GD, Singaas EL (2007) Fitting photosynthetic carbon dioxide response curves for C3 leaves. *Plant, Cell Environ* 30:1035–1040. <https://doi.org/10.1111/j.1365-3040.2007.01710.x>
- Singh SK, Badgajar GB, Reddy VR, Fleisher DH, Timlin DJ (2013) Effect of phosphorus nutrition on growth and physiology of cotton under ambient and elevated carbon dioxide. *J Agron Crop Sci* 199:436–448. <https://doi.org/10.1111/jac.12033>
- Singh SK, Reddy VR, Fleisher DH, Timlin DJ (2019) Interactive effects of temperature and phosphorus nutrition on soybean: leaf photosynthesis, chlorophyll fluorescence, and nutrient efficiency. *Photosynthetica*. 57(1):248–257. <https://doi.org/10.32615/ps.2019.036>
- Tantray AY, Ali HM, Ahmad A (2020) Analysis of proteomic profile of contrasting phosphorus responsive rice cultivars grown under phosphorus deficiency. *Agronomy* 10(7):1028. <https://doi.org/10.3390/agronomy10071028>
- Thalman M, Santelia D (2017) Starch as a determinant of plant fitness under abiotic stress. *New Phytol* 214:943–951. <https://doi.org/10.1111/nph.14491>
- Veneklaas EJ, Lambers H, Bragg J, Finnegan PM, Lovelock CE, Plaxton WC, Price CA, Scheible WR, Shane MW, White PJ, Raven JA (2012) Opportunities for improving phosphorus-use efficiency in crop plants. *New Phytol* 195:306–320. <https://doi.org/10.1111/j.1469-8137.2012.04190.x>
- Win M, Nakasathien S, Sarobol E (2010) Effects of phosphorus on seed oil and protein contents and phosphorus use efficiency in some soybean varieties. *Kasetsart J - Nat Sci* 44:1–9

- Yan N, Zhang YL, Xue HM, Zhang XH, Wang ZD, Shi LY, Guo DP (2015) Changes in plant growth and photosynthetic performance of *Zizania latifolia* exposed to different phosphorus concentrations under hydroponic condition. *Photosynthetica* 53:630–635. <https://doi.org/10.1007/s11099-015-0149-7>
- Yang JT, Preiser AL, Li Z, Weise SE, Sharkey TD (2016) Triose phosphate use limitation of photosynthesis: short-term and long-term effects. *Planta* 243:687–698. <https://doi.org/10.1007/s00425-015-2436-8>
- Zhang D, Song H, Cheng H, Hao D, Wang H, Kan G, Jin H, Yu D (2014) The acid phosphatase-encoding gene *GmACP1* contributes to soybean tolerance to low-phosphorus stress. *PLoS Genet* 10:8–10. <https://doi.org/10.1371/journal.pgen.1004061>
- Zhang H, Yang Y, Sun C, Liu X, Lv L, Hu Z, Yu D, Zhang D (2020) Up-regulating *GmETO1* improves phosphorus uptake and use efficiency by promoting root growth in soybean. *Plant Cell Environ* 43(9):2080. <https://doi.org/10.1111/pce.13816>
- Chu S, Li H, Zhang X, Yu K, Chao M, Han S, Zhang D (2018) Physiological and proteomics analyses reveal low-phosphorus stress affected the regulation of photosynthesis in soybean. *Int J Mol Sci* 19:. <https://doi.org/10.3390/ijms19061688>
- El-Mejjaouy Y, Lahrir M, Naciri R, Zeroual Y, Mercatoris B, Dumont B, Oukarroum A. How far can chlorophyll a fluorescence detect phosphorus status in wheat leaves (*Triticum durum* L.), *Environ Exp Bot*. <https://doi.org/10.1016/j.envexpbot.2021.104762>
- EMBRAPA 2021. Soja em números (safra 2020/21). Empresa Brasileira de Pesquisa Agropecuária. Available via: <https://www.embrapa.br/web/portal/soja/cultivos/soja1/dados-economicos>. Accessed 11 Jul 2022.
- Genty B, Harbinson J (1996) Regulation of light utilization for photosynthetic electron transport. *Photosynth Environ* 67–99. [https://doi.org/10.1007/0-306-48135-9\\_3](https://doi.org/10.1007/0-306-48135-9_3)
- Hodge JE (1962) Determination of reducing sugars and carbohydrate. *Methods Carbohydr Chem* 380–394
- Irf M, Az T, Aamer M, B HM, Kadambot HMS, Xu M (2020) Phosphorus (P) use efficiency in rice is linked to tissue-specific biomass and P allocation patterns. 1–14. <https://doi.org/10.1038/s41598-020-61147-3>
- Malhotra H, Vandana, Sharma S, Pandey R (2018) Phosphorus nutrition: plant growth in response to deficiency and excess. In: *Plant Nutrients and Abiotic Stress Tolerance*. Springer Singapore, Singapore, pp 171–190
- Moller MRF, Viégas I de JM, Matos A de O, Parry MM (1997) *Análises de Tecido Vegetal: Manual de Laboratório*
- Yang A, Kong L, Wang H, Yao X, Xie F, Wang H, Ao X (2020) Response of soybean root to phosphorus deficiency under sucrose feeding: insight from morphological and metabolome characterizations. *Biomed Res Int* 2020. <https://doi.org/10.1155/2020/2148032>
- Zogli P, Pingault L, Libaut M (2017) Physiological and molecular mechanisms and adaptation strategies in soybean (*Glycine max*) under phosphate deficiency. In: Sulieman S, Tran LSP (eds.) *Legume nitrogen fixation in soils with low phosphorus availability*. Springer, Cham. pp. 219–242. <https://doi.org/10.1007/978-3-319-55729-8>

**Publisher's Note** Springer Nature remains neutral with regard to jurisdictional claims in published maps and institutional affiliations.